RESILIENT INFRASTRUCTURE
June 1–4, 2016
RESILIENT INFRASTRUCTURE LONDON 2016

FINITE ELEMENT MODELLING OF COMPOSITE HOLLOWCORE SLABS

Aiham Adawi
Western University, Canada

Maged A. Youssef
Western University, Canada

Mohamed E. Meshaly
Alexandria University, Egypt

ABSTRACT

Hollowcore slabs are commonly used for floor and roofs of residential and commercial buildings. Concrete topping, which is commonly cast for leveling purposes, can also be used to increase the load capacity of hollowcore slabs. The post-cracking behaviour of hollowcore slabs greatly affects their ultimate strength. The composite action adds another level of nonlinearity. This paper presents a comprehensive 3-D finite element model that can predict the behaviour of such composite slabs. Nonlinear springs were used to model the interface layer. The nonlinear material behaviour of the concrete and the prestressing strands were also accounted for. Innovative analysis technique to simulate the staged construction of composite hollowcore slabs is also presented. The proposed analysis is validated using results from a previous experimental study by the authors.

Keywords: hollowcore slabs, composite behaviour, interface properties, 3-D nonlinear finite element analysis.

1. INTRODUCTION

The vast majority of previous literature on the composite action of flexural elements is related to steel beams, where the concrete topping is attached to the top flange of the steel beam using shear connectors. In such cases, the connectors (shear studs) can be modeled using spring elements (Salari et al., 1998; Queiroz et al., 2006). The stiffness (force-displacement curve) of those springs is usually evaluated through series of push-off tests. Deng (2012) provided a modeling technique that accounted for the behaviour of shear studs in composite prestressed concrete girders and composite steel girders.

Number of researchers successfully modeled non-composite hollowcore slabs using finite element analysis. To the authors' knowledge, there is a lack of nonlinear numerical models in the area of composite hollowcore slabs. Mones (2012) conducted multiple push-off tests on composite hollowcore slabs with different surface finishes. Mones (2012) also modeled the composite behaviour of hollowcore slabs using 2-D plane-stress elements. Spring elements resembled the interfacial shear stress. The analysis assumed linear-elastic behaviour and did not account for the peel behaviour. The shear stiffness of the spring elements was determined based on the results of the push-off tests, which resembled a state of pure shear. Results of the finite element analysis were not validated.

The behaviour of the concrete material becomes highly nonlinear after cracking, which greatly affects its overall response. Therefore, it is necessary to investigate the behaviour of composite hollowcore slabs in the post-cracking zone. This paper presents a 3-D nonlinear finite element model for a composite hollowcore slab specimen. The slab was part of a comprehensive experimental program conducted by the authors at Western University, Canada (Adawi et al, 2015). Interface stiffness values obtained from the push-off tests presented by Adawi et al. (2015) were used as initial values in the modeling of the full-scale slab. The final non-linear interfacial shear and peel stiffnesses of the

composite slab were then evaluated. The actual shear stress distribution along the interface between the hollowcore slab and the concrete topping was then evaluated.

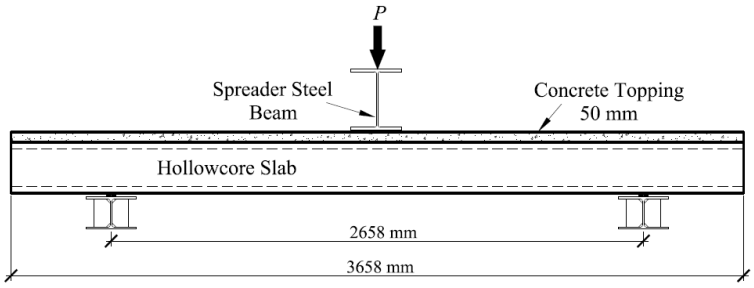

(a) Full-scale test setup.

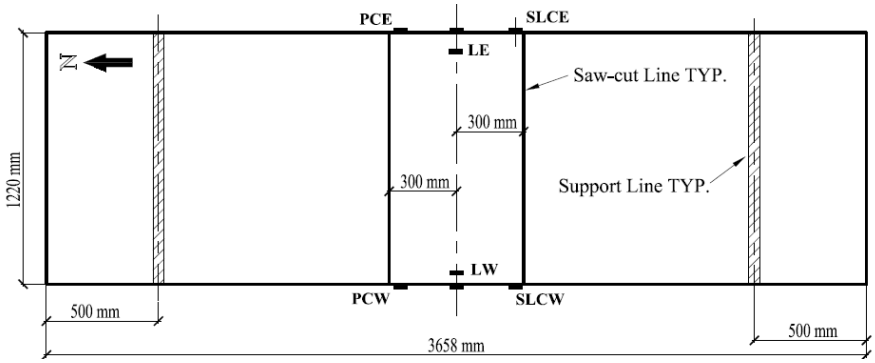

(b) Instrumentation.

(c) Test photo

Fig. 1: Full-scale test

2. FULL-SCALE TEST

The tested composite hollowcore slab (FMA2-2C) had a thickness of 203 mm, a machine-cast surface finish, and 7-1/2" low-relaxation prestressing strands with ultimate nominal tensile strength of 1860 MPa. The concrete compressive strength of the slab was 50 MPa. The length and width of the tested slab were approximately 3658 mm and 1220 mm, respectively. The concrete topping had a thickness of 50 mm and a concrete compressive strength of 30 MPa. Fig. 1 shows the full-scale test setup and the instrumentation. The concrete topping was saw-cut as shown in Fig. 1(b) to induce higher interfacial shear stresses during the test. The load (*P*) was applied at mid-span using a steel spreader beam. Vertical deflection was measured at mid-span using the displacement gauges: LE and LW. Slip was measured on both sides of the concrete topping using SLCW and SLCE. Peel deformations were measured using PCW and PCE. Strain gauges were also attached to the hollowcore slabs (SHCE and SHCW) and the concrete topping (STE and STW) at mid-span. The composite slabs were loaded at mid-span by increasing the load at 10 kN per minute up to failure. More details about the full-scale test are given in Adawi et al. (2015).

3. FINITE ELEMENT MODELING

ANSYS R15.0 (2013) was utilized to model the full-scale test. This section explains the modeling techniques including modeling of the prestressing force and the staged construction process. The material models used in the analysis will then be presented.

The full-scale test was conducted using a three-point bending test setup as shown in Fig. 1. The finite element idealization of the test is demonstrated in Fig. 2. The main components of the full-scale test are: the hollowcore slab, the concrete topping and the interface between the hollowcore slab and the concrete topping. 6-noded and 8-noded 3-D solid elements (SOLID65) were used to model the hollowcore slab and the concrete topping, respectively. The interface layer between the hollowcore slab and the concrete topping was modeled using nonlinear spring elements. A typical 3-D model for the composite hollowcore slab is shown in Fig. 3(a).

The prestressing strands were modeled using a 3-D truss element (LINK180) that has two nodes with three translational degrees of freedom at each node. The geometry of a typical composite hollowcore slab was initially created by using block shapes. Several ANSYS geometry tools including "BOOLEANS" were used to create the voids in the hollowcore slab. The meshing was first conducted on the cross section area using the generic area element (MESH200) as shown in Fig. 6. The meshed cross section was then swept over the entire hollowcore slab's using the (SOLID65) concrete element. Aspect ratio adequacy was verified automatically using the ANSYS recommended built-in criteria.

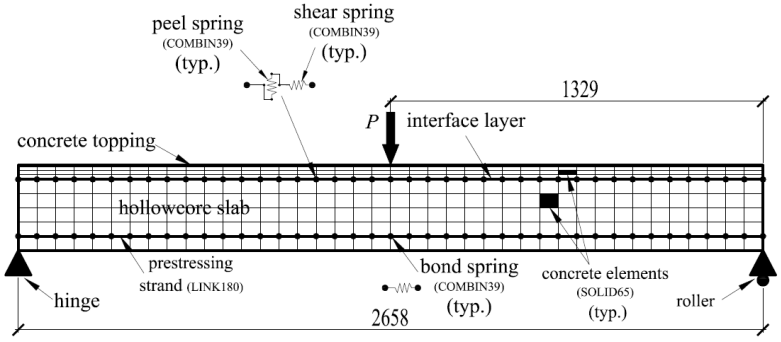

Fig. 2: FE idealization of the full-scale test.

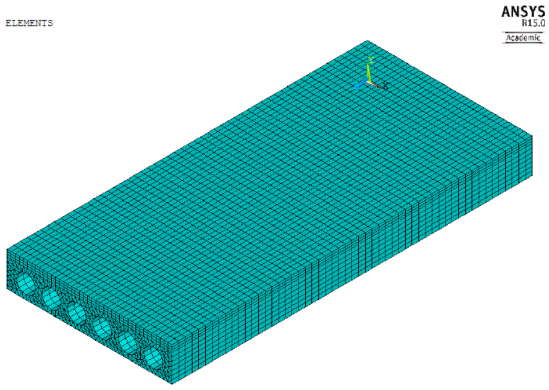

(a) General 3-D view of the composite hollowcore slab.

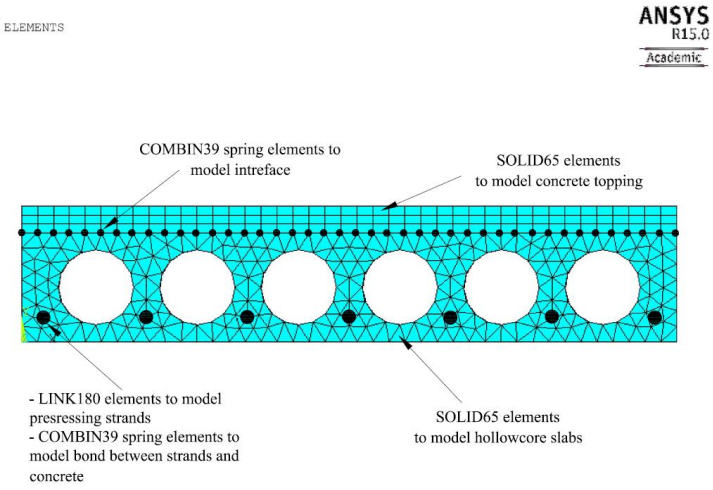

(b) Cross section of the composite slab.

Fig. 3: Finite element model of the full-scale test

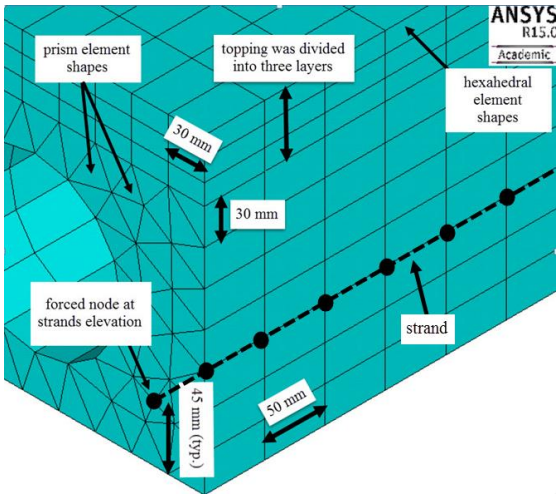

Fig. 4: Meshing layout.

The coincident nodes at the interface were connected using nonlinear spring elements (COMBIN39). The boundary conditions were assigned such that they simulate the actual support conditions of the composite slab in the full-scale test, Fig. 2. The bottom nodes at the hinged end of the slab were restricted in the Z and Y directions while the nodes at the roller support were only restricted in the Y direction. The load, (P), was applied at the midspan nodes located at the top of the concrete topping. Each strand consisted of a number of LINK180 elements that have the same length as the concrete elements along the Z direction, Fig. 4.

3.1 Special Modeling Techniques

Modeling the composite hollowcore slab involves dealing with two complex issues: the transfer of the prestressing force and the strain discontinuity between the hollowcore slab and the concrete topping. The concrete topping was cast after the hollowcore slab. This implies that the strains, and stresses, in the concrete topping were equal to zero before applying the concentrated load (*P*) shown in Fig. 2. The following sections explain how those two issues were addressed.

3.3.1 Prestressing Force

The prestressing force was modeled using the "initial state" (INISTATE) command. This command can be used to apply specific strain values to element LINK180 that resembles the strands. The strain in the strands at the time of testing was estimated at 0.0055. The jacking stress was 70% of the strand's ultimate tensile strength. Prestress losses were estimated to be 15% of the jacking stress. Bond between the hollowcore slab and the prestressing strands was modeled using nonlinear spring elements (COMBIN39), as shown in Fig. 5. The constitutive force-displacement curve for those springs was developed using the bond-slip model by Balázs (1992), Eq. (1). The bond stress (τ_b) is multiplied by the cylindrical circumferential area of the strand along the segment length to define the spring force at different slip values.

[1] $$\tau_b = 2.324 \times \sqrt{f'_{ch}(s)^{1/2}} \quad \text{(MPa)}$$

Where (τ_b) is the bond stress in the direction of slip, (f'_{ch}) is the concrete compressive strength of the hollowcore slab, and (s) is the slip between the strand and the surrounding concrete in millimeters.

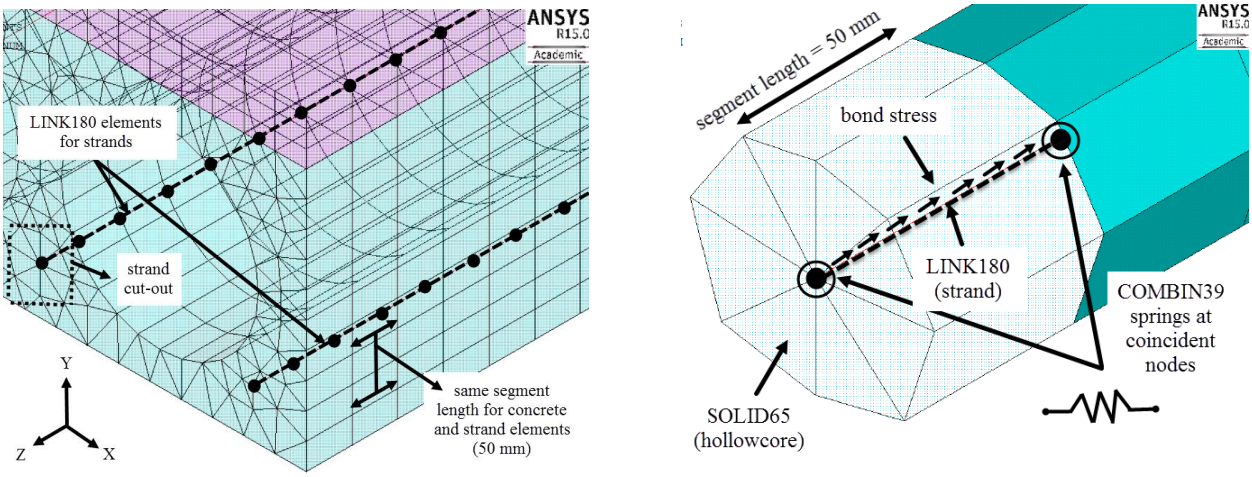

(a) Modeling of strands.

(b) Location of bond springs.

Fig. 5: Illustration of the bond-stress modeling.

3.3.2 Strain Discontinuity

The concrete topping was cast after prestressing the hollowcore slab. Accordingly, the strains and stresses in the concrete topping were equal to zero before applying the external load (*P*). The interfacial shear and peel stresses were also equal to zero at that stage. Fig. 6 illustrates the staged construction process for composite hollowcore slabs. To model this process, the initial stiffness of the concrete topping was significantly reduced such that it does not contribute to the overall stiffness. This was achieved by using the "Kill" feature in ANSYS. The prestressing force was then applied as an initial strain using the "Initial State" feature. Finally, the stiffness of the concrete topping was activated to reflect its actual value using the "Birth" feature. The concrete topping and the interface springs were checked to ensure that they did not experience any stresses during the prestressing process before applying the load (*P*) along the entire width of the composite slab as shown in Fig. 7.

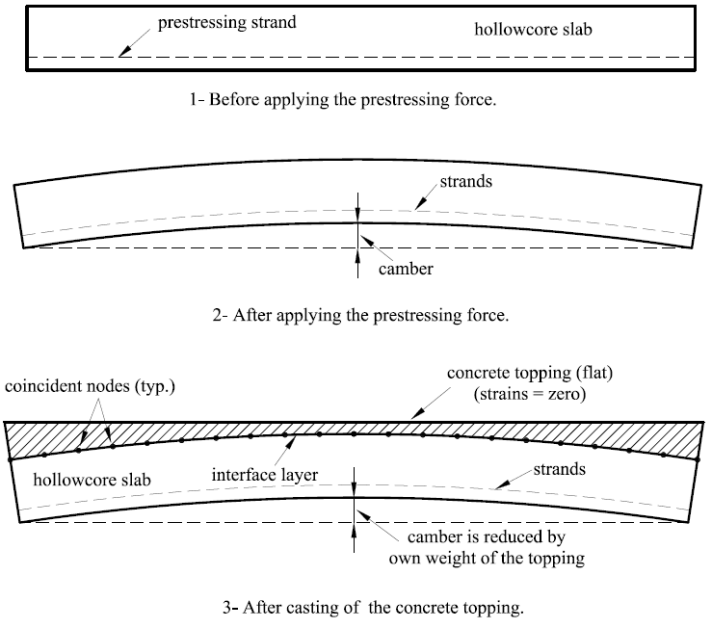

Fig. 6: Staged construction steps.

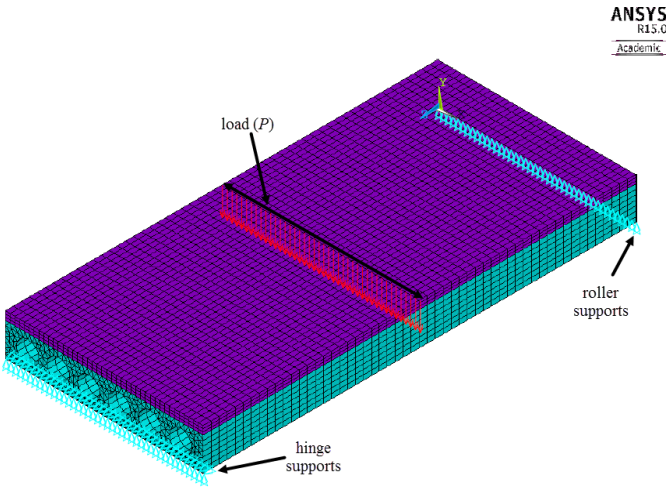

Fig. 7: Loaded composite slab

4. MATERIAL MODELS

4.1 Concrete

The linear isotropic component was defined by the concrete initial tangent stiffness (E_c) that was taken equal to ($3320\sqrt{f'_c}+6900$ MPa) as recommended by Collins (1991). Poisson's ratio was taken equal to 0.2. The unconfined concrete stress-strain relationship Eq. (2), which was proposed by Popovics (1973) and calibrated by Porasz (1989), was used to define the multilinear stage. Shear transfer coefficients were taken as 0.30 and 0.95 for open and closed cracks, respectively (Cheng and Wang, 2010). The uniaxial tensile cracking stress (f_t) was calculated using the formula recommended by Bentz (2000), Eq. (3).

[2] $$f_c = f'_c \frac{n(\varepsilon_c/\varepsilon'_c)}{n-1+(\varepsilon_c/\varepsilon'_c)^{nk}} \text{ (MPa)}$$

[3] $$f_t = 0.45\left(f'_c\right)^{0.4}$$

Where

$$n = 0.8+\frac{f'_c}{17}$$

$$k = \begin{cases} 1 & (\varepsilon_c/\varepsilon'_c)<1.0 \\ 0.67+\dfrac{f'_c}{62} & (\varepsilon_c/\varepsilon'_c)>1.0 \end{cases}, \quad \varepsilon'_c = \frac{f'_c\, n}{E_c(n-1)}$$

f_c: concrete compressive stress, ε_c: concrete compressive strain, f'_c: peak cylinder compressive strength, ε'_c: strain at peak compressive stress, n: curve fit parameter, k: factor to account for the post peak ductility of high strength concrete.

4.2 Prestressed Reinforcement

The stress-strain curve for the strands was constructed using the Ramberg-Osgood formulation (Collins, 1991) shown in Eq. (4).

[4] $$f_p = E_p\varepsilon_p\left\{A+\frac{1-A}{\left[1+\left(B\varepsilon_p\right)^C\right]^{\frac{1}{C}}}\right\} \le f_{pu}$$

Where (f_p) and (ε_p) are the stress and strain in the prestressing strand, respectively. The constants A, B and C were taken as 0.025, 118 and 10.0, respectively, as recommended in the 4th edition of the Canadian Precast/Prestressed Institute (CPCI) design manual (2007). The modulus of elasticity (E_p) was taken as 200,000 MPa.

5. FAILURE CRITERIA

The failure criteria were: (1) maximum principal compressive concrete strain of 0.002 indicating shear failure; (2) longitudinal compressive strain of 0.0035 indicating flexural failure; (3) strands' tensile stress of 1860 MPa; (4) force in shear springs reaching their capacity indicating interface shear failure; and (5) force in peel springs reaching their capacity indicating interface peel failure.

6. FINITE ELEMENT ANALYSIS RESULTS

The load-deflection results obtained from the experimental test and the FEA analysis are shown in Table 1. The results are also shown graphically in Fig. 8. It can be noticed that the finite element analysis was fairly successful in

capturing the behaviour of the slab in terms of stiffness and failure load. The tested slab had a cut in its concrete topping and failed because the compressive strains in the hollowcore slab exceeded the limit of 0.0035. This failure followed the horizontal shear failure. The significant ductile behaviour observed experimentally is due to the confining effect of the applied load. The strains show good agreement between the experimental and the FEA results as shown in Fig. 9. The strain relaxation in the concrete topping after cracking was successfully captured in the FEA as shown in the graphs.

Table 1: Load-deflection results

Slab Label	Analysis Type.	Cracking load, kN	Failure load, kN	Deflection at failure, mm	Failure Type
FMA2-2C	Exp.	152	244	49.6	concrete crushing
	FEA	164	206	18.4	concrete crushing

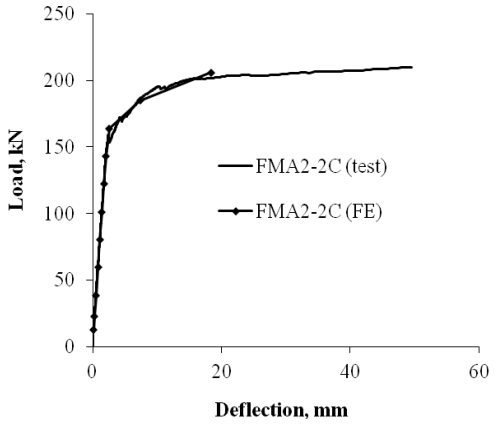

Fig. 8: Load-deflection results.

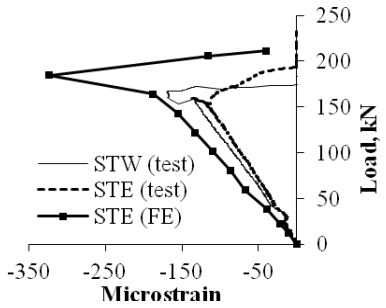

Fig. 9: Mid-span strain Results

The stiffness of the nonlinear springs (COMBIN39) simulating the interface between the hollowcore slab and the concrete topping was crucial in the FEA analysis. The constitutive force-displacement curves were initially based on the FEA results of the push-off tests. The final force-displacement curves were determined using an extensive iteration process to match the full-scale experimental results. The final shear and peel stiffness results along with the parameters defining the force-displacement curves for the interface springs are show in Table 2 and Fig. 10. Difference between these values and the push-off test values can be attributed to the effect of confinement of the

interface layer that resulted from the applied load and the interaction between the shear and peel stresses along the interface layer.

Table 2: FEA shear and peel stiffness results

Slab Label	Shear Stiffness				Peel Stiffness			
	yield		Ultimate		yield		ultimate	
	P_y, N	Slip, mm	P_u, N	Slip, mm	P_y, N	Peel, mm	P_u, N	Peel, mm
FMA2-2C	2740	0.007	6170	0.24	1000	0.5	1000	0.5

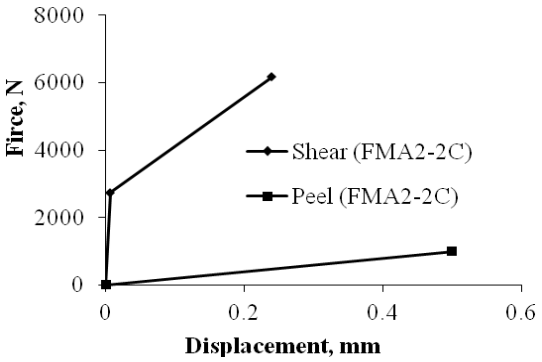

Fig. 10: Interfacial springs properties

When the concrete topping length is reduced for the tested slab (FMA2-2C), the shear stress intensifies causing the nonlinear behaviour to become apparent. The maximum interfacial shear stiffness evaluated from the FEA reached 261 (N/mm)/mm^2 during the full-scale test. The interfacial peel stiffness was found to be approximately 1.3 (N/mm)/mm^2.

The shear stress distribution along the interface between the hollowcore slab and the concrete topping for tested slab is shown in Fig 11. The yielding load is the load at which the composite slab stiffness changes from linear to nonlinear based on the load-deflection curve of the slab.

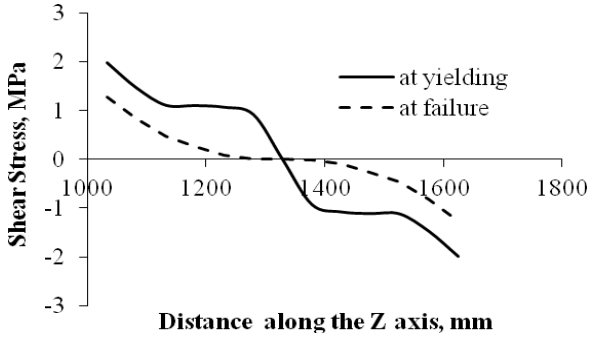

Fig. 11: Interfacial shear stress distribution.

Considering the full-scale test setup, where there is only one point load at mid-span, the maximum interfacial shear stress occurs at the end of the slab where the moment is equal to zero and the vertical shear is at maximum. The shear stress dissipates towards the mid-span section, where the moment is maximum and the vertical shear is equal to zero. It is apparent that the tested slab had sustained shear stresses higher than the 0.55 MPa and 0.7 MPa limits set by the ACI 318-08 (2008) and the CSA A23.3-04 (2004) design standards.

7. CONCLUSIONS

Modeling of a composite hollowcore slab full-scale test using the finite element method was conducted in this paper. The FEA showed comparable results with the experimental program conducted by Adawi et al. (2015). This demonstrates that the presented FEA approach and modeling procedures are adequate in capturing the behaviour of composite hollowcore slabs with an acceptable accuracy.

When the concrete topping is reduced, apparent nonlinear behavior of the shear and peel stiffness was observed. Confinement provided by the applied load is believed to have significantly increased the interface stiffness. This suggests that live loads tend to confine the interface layer in the area where they are applied producing a more ductile behavior before failure. Considering the first stiffness branch of the FEA results, the shear stiffness of the tested composite hollowcore slab was 261 $(N/mm)/mm^2$ while the peel stiffness was found to be 1.3 $(N/mm)/mm^2$.

REFERENCES

ACI 318. 2008. *Building code requirements for structural concrete (ACI 318-08) and commentary*. American Concrete Institute, Michigan, United States.

Adawi A, Youssef MA, Meshaly M, 2015. Experimental investigation of the composite action between hollowcore slabs with machine-cast finish and concrete topping. *Engineering Structures*, 91, pp. 1-15.

ANSYS® Academic Research, Release 15.0, 2013, ANSYS, Inc.

Balázs, GL. 1992. Transfer control of prestressing strands. *PCI journal*. 37(6), 60–71.

Bentz, E.C., 2000. *Sectional Analysis of Reinforced Concrete*. PhD Thesis, Department of Civil Engineering, University of Toronto.

Cheng, S. and Wang, X.. 2010. Impact of Interaction between Adjacent Webs on the Shear Strength of Prestressed Concrete Hollow-Core Units. *PCI Journal*. Vol. 55, No. 3, pp. 46-63.

Collins, M.P. and Mitchell, D.. 1991. *Prestressed Concrete Structures*. Prentice-Hall, 760 pp.

CSA A23.3. 2004. *Design of concrete structures (A23.3-04)*. Mississauga, ON, Canada: Canadian Standard Association (CSA).

Deng, Yaohua. 2012. *Efficient Prestressed Concrete-Steel Composite Girder for Medium-Span Bridges*. PhD Thesis, University of Nebraska-Lincoln, Lincoln, NE, United States.

Mones, R.M.. 2012. *Interfacial Strength Between Prestressed Hollow Core Slabs and Cast-in-Place Concrete Toppings*. M.E.Sc. Thesis. University of Massachusetts, Amherst, Massachusetts, United States.

Popovics S. 1973. A Numerical Approach to the Complete Stress-Strain Curve of Concrete. *Cement and Concrete Research*. Vol. 3, pp. 583-599.

Porasz, A. 1989. *An Investigation of the Stress-Strain Characteristics of High Strength Concrete in Shear*. M.A.Sc. Thesis, University of Toronto.

Queiroz F.D., Vellasco P.C.G.S and Nethercot D.A.. 2007. Finite element modeling of composite beams with full and partial shear connection. *Journal of Constructional Steel Research*. 63 (2007), pp. 505-521.

Salari M. R., Spacone E., Benson P. and Frangopol D.M.. 1998. Nonlinear Analysis of Composite Beams with deformable Shear Connectors. *Journal of Structural Engineering (ASCE)*. October 1998, pp. 1148-1158.

Willam, K.J. and Warnke, E.P.. 1974. Constitutive Model for Triaxial Behaviour of Concrete. Seminar on Concrete Structures Subjected to Triaxial Stresses. *International Association of Bridge and Structural Engineering Conference*. Bergamo, Italy, p.174.